

Integrated Solutions Deliver Improved Wellbore Integrity

Greg Mullen, Keith Browning, Edgar Luna, David Schwertner and Chris Wolfe, Baker Hughes Incorporated

Copyright 2010, AADE

This paper was prepared for presentation at the 2010 AADE Fluids Conference and Exhibition held at the Hilton Houston North, Houston, Texas, April 6-7, 2010. This conference was sponsored by the Houston Chapter of the American Association of Drilling Engineers. The information presented in this paper does not reflect any position, claim or endorsement made or implied by the American Association of Drilling Engineers, their officers or members. Questions concerning the content of this paper should be directed to the individuals listed as authors of this work.

Abstract

Controlling costs and mitigating risk make wellbore integrity a major priority for global operators. The location and type of well determines which barriers they must overcome in order to successfully complete a drilling campaign. Mature deepwater reservoirs, exploratory wells, high-pressure / high-temperature (HP/HT) and extended reach (ERD) wells all pose their own unique challenges. Each of these obstacles must be addressed effectively and efficiently. This paper discusses an integrated solutions approach to use best-available technology to meeting the challenges presented. The technology offering is segmented and focuses on the appropriate solutions package designed to the specific needs of an operation.

The paper will discuss various wellbore integrity issues and present the efficiency of these solutions through this integrated approach. A case history will be presented that demonstrates quantifiable benefits to the customer.

Introduction

Operators have significant investments in onshore and deepwater facilities that require efficient removal of hydrocarbons to justify the economics of a project. Significant cost overrun due to non-productive time (NPT) associated with wellbore stability problems can diminish margins that turn a potential profitable project to minimum returns.

As fields mature, drilling through depleted zones to reach deeper reservoirs is necessary and many times costly. Stuck pipe, mud losses, twist-offs and loss of wellbore are possible. Significant drops in pore pressure associated with hydrocarbon recovery can weaken reservoir rock while the adjacent low permeable rock (shale) often retains its original pore pressure. Drilling through the shale requires sufficient pressure to prevent wellbore collapse; however there is high potential for severe mud losses due to formation breakdown in the depleted zones. This scenario can require significant time and expense to overcome.

Solutions for drilling through depleted zones to access deeper hydrocarbon bearing reservoirs include techniques such as expandable liner, drilling with casing and managed pressure drilling. These techniques are costly and are not always successful.

Wellbore strengthening while drilling is a concept that has been around for many years and has been time tested and field

proven many times over. In 2004, Alberty et al. presented the concept of stress cage for wellbore strengthening in sand formations. He concluded that high elevated stresses in the near wellbore region can be created by opening small fractures that are propped open and plugged with high compressive strength bridging particles.^[1] Aston et al. presented a "designer mud" approach to increase fracture resistance while drilling in shale and sandstone. Results from their field trials in shale, sand/shale and sand formations were presented. They reported an increase of 5.4 pounds per gallon (ppg) in formation breakdown pressure in a shale formation.^[2] In 2006, Benaissa et al. presented a case history on wellbore strengthening in South Texas by using a "deformable sealant." This application was in the low permeable (0.1 to 150 mD) Wilcox formation. Their approach was to create an internal filter cake with a micronized sealing polymer resulting in blockage of pore pressure transmission. They presented results from formation integrity tests (FIT), which showed an increase of 1.16 ppg.^[3]

This paper will discuss an integrated approach to help mitigate NPT due to whole mud losses in depleted zones. A new software package will be introduced that is capable of performing geomechanics analysis that predicts fracture pressure and width. If necessary, it then calculates the optimum blend of bridging material for a particular fracture width. The software use is intended to assist operators during preplanning and execution of drilling projects, by predicting the occurrence of fractures and proposing an optimum product blend for wellbore strengthening. The software does not replace full-scale geomechanics studies.

An Integrated Approach for Wellbore Stability

Preplanning drilling projects require knowledge of the field in which the well(s) will be drilled. There are circumstances where operators require a complete geomechanics study: fields that are tectonically stressed or mature highly depleted fields are typical candidates to conduct a full geomechanics study. Conducting such studies is time consuming, expensive and in many cases, particularly for small independent operators, cost prohibitive. The integrated approach described in this paper can facilitate timing versus a full-scale study; however the physics within the software presented is recognized as industry standard. A standard approach in preplanning drilling projects is to thoroughly review all available offset well data from which estimates on

mud weight windows identify loss zones and kick events, tight spots, washouts and other potential problems experienced. Information from formation evaluation logs, wireline logs and downhole tool data are invaluable for preplanning drilling projects and populating engineering software.

From these data sources, information on pore and fracture pressures, minimum horizontal stress, azimuth of maximum horizontal stress, overburden stress and rock properties can be estimated.

The integrated approach to wellbore stability includes:

- Temperature modeling to populate hydraulics and geomechanics model
- Hydraulics modeling to populate geomechanics model
- Offset research for pore / fracture pressures and rock property estimations
- Geomechanics modeling to determine wellbore collapse / fracture pressures and fracture width
- Bridging material for wellbore strengthening

Figure 1 illustrates the procedures to an integrated approach for wellbore stability. Once the rock properties and formation stresses are determined from offset data review, or are customer supplied, an iteration process to determine the optimum mud viscosity, mud temperature, equivalent static density (ESD) and ECD is performed to eliminate or minimize potential fracture openings. When fractures are predicted, an optimum particle-size-distribution (PSD) formulation is calculated with the bridging software. The method described uses field validated hydraulics and temperature software to populate the geomechanics model.

Geomechanics Modeling

The geomechanical model was developed in-house and is based on the linear elastic model. The model is capable of computing the collapse pressure (the minimum downhole pressure needed to avoid borehole shear failure) and the formation breakdown pressure (FBDP), which is the maximum downhole pressure that can be applied before hydraulic fracturing occurs. Currently, the program computes the collapse pressure based on three shear failure criteria: Mohr-Columb, Drucker-Prager and Modified Lade. In addition, the program also yields fracture geometry predictions based on the Perkins-Kern-Nordgren (PKN), Khristianovic- Geertsma-de Klerk (KGD) and modified KGD models.

The model requires nine formation stress and rock property data inputs to run a simulation. See **Table 1** for a complete list of input parameters and results. Several modes of analysis are available; the user can perform a single point analysis or a batch mode where multiple depths are evaluated. Additional features include the ability to perform a sensitivity analysis by varying quantities over a predetermined range. For example, when uncertainties exist on values such as Young's modulus or pore pressure, minimum, maximum and decrement values can be entered. The results are then presented in graphical format.

Another feature allows the user to determine a "drillability matrix." A range of wellbore inclination and azimuth are input by the user and the resulting output is a matrix displaying minimum required mud weights and formation breakdown pressures on a per degree increment.

Examples of the geomechanical model output are shown in Figures 2-5. **Figure 2** shows a sensitivity analysis over a range of pore pressures from 4.7 ppg to 3.7 ppg. This example also shows the dependency of the FBDP (left axis) on S_h (minimum horizontal stress) and range of pore pressures. The maximum fracture width (μ), as predicted by the modified KGD model, is also shown. **Figure 3** shows the same sensitivity analysis with Young's modulus as the variable. **Figure 4** is an example of a drillability matrix. The results presented are the maximum allowable ECD calculated for each hole angle / azimuth combination. In this example, the wellbore angle / azimuth varies from 25 to 45° / 270 to 277°, respectively. A second matrix shows results for minimum allowable mud weight. **Figure 5** shows results over an interval. Results displayed on the plot are FBDP, S_h , minimum mud weight, pore pressure and ECD. A second plot shows the predicted fracture width versus depth.

Temperature Modeling

Temperature affects on viscosity and density of invert emulsion drilling fluids can be significant. The importance to measure viscosity and calculate density of compressible fluids under downhole pressures and temperatures has been documented by many authors.^[6-8] Drilling fluid viscosities are measured on HP/HT viscometers while density corrections are calculated with a compositional model.^[7]

Temperature effects on rock strength should be considered as well. Mud losses usually occur after trips while breaking circulation. In 2001, Jones et al. noted that most losses had occurred when breaking circulation with cold and gelled up mud. This was measured by downhole pressure tools that showed a 0.5-ppg difference in the ECD between warm and cold mud. They expressed additional concerns that the cold mud probably reduced the formation fracture gradient.^[4] Gonzalez et al. conducted a full-scale field experiment with water-based mud. In this study, leak-off tests (LOTs) were performed at three temperatures: 92°F, 133°F and 153°F. Their results showed an improvement of 1.5 ppg in the effective fracture gradient with a mud temperature of 92°F compared to 153°F. An increase of 0.8 ppg was noted from 92°F compared to 133°F. They suggested that temperature models coupled with wellbore stability models and pressure prediction models should be considered to allow for real-time determination of the dynamic pressure profile that exists in wellbores as a result of changing wellbore temperatures.^[5]

Accurate determination of temperature is the most important parameter for pre-well planning and during the drilling operation as temperature can affect many drilling parameters. The benefits are numerous and include: accurate downhole pressures while drilling and completing, surge and swab pressures, wellbore stability, ballooning, tripping

schedules, tool life, mud cooler requirement, hydrate prediction and cement design. Additionally, insight into potential problems can help plan for rigsite product inventories such as bridging products for losses and wellbore strengthening.

The temperature model presented in this paper is a dynamic model. It was introduced in the early 1990s as an HP/HT pressure and temperature model. Enhancements to address non-HP/HT wells such as deepwater wells have been made.

The model allows for heat generated in the system from mechanical energy and hydraulic energy. Heat flow due to forced convection, conductive and natural conduction is considered.^[9] Thermophysical properties of all components including the formation, steel components, cement and drilling mud are considered. The drilling fluid thermophysical properties are calculated based on mud composition. Thermophysical properties can be user defined to simulate insulated pipe, risers and “tune” drilling fluid to match known conditions.

The model is capable of running batch modes that simulate actual drilling operations. For example, in pre-well planning a batch mode could be set to drill a ninety-foot stand at thirty ft/hr for three hours followed by a 20-minute connection. **Figures 6 and 7** show results of a circulating temperature profile (CTP) and flow rate. The flow rate graph illustrates when drilling commenced and then ceased when making a connection.

Hydraulic Modeling

Hydraulics modeling or downhole pressure predictions are an obvious necessity for pre-planning and during the execution phase of a project. The accuracy of hydraulics modeling is greatly dependent on the accurate prediction of downhole temperatures, pressures and pressure losses.^[10]

Pressure-volume-temperature (PVT) data for each unique base fluid should be measured and incorporated into the hydraulics model for accurate density predictions. **Tables 2 and 3** list typical PVT data for a low toxicity mineral oil (LTMO) and a whole mud with a 78:22 oil/water ratio (OWR). The base fluid density varies by as much as 14% and the whole mud density varies by 6%.

Accurate downhole pressure predictions under static and circulating conditions are necessary in determining whether the well can withstand the required flow rates necessary to ensure sufficient cuttings removal, supply enough hydraulic horsepower to the bit and stay within standpipe pressure limits. Additionally, wellbore stability models require the maximum pressure the wellbore will be exposed (ECD or surge pressures) to determine if formation breakdown occurs and the ESD to determine if a fracture will remain open under static conditions. With this knowledge, design changes in the drilling fluid can be made to prevent formation breakdown or bridging material can be formulated to strengthen the wellbore.

Bridging

The bridging material design software contains four bridging rules: Abrams 1/3 rule, Kaeuffer square root rule, Fracture rule (D-90 rule) and Vickers Rule.^[11] With determined pore size or fracture width, the model calculates an optimal product mix. The software considers all products in the data base as well as the PSD of the drilling fluid. **Figure 8** shows a PSD fit for a neat pill, without the drilling fluid PSD considered. **Figure 9** shows results with the drilling fluid PSD included. Additional output includes the % in range and the square root rule results.

A “slot sealing” test was developed to evaluate lost circulation packages’ effectiveness in bridging fractures. The test equipment was designed with an adjustable slot assembly to allow simulation of varying fracture widths (up to 3000 microns) and capable of pressures up to 4000 pounds per square inch (psi). **Figures 10 and 11** show the adjustable slot assembly.

LCM Recovery

Drilling fluids continue to be engineered for wellbore stability through the use of specifically sized particles. These particles may be conventional lost circulation materials used to reduce downhole losses, or sized material added to bridge fractures and pore spaces. This practice allows higher fluid densities (often above the fracture gradient) to be added, resulting in:

- Reduced whole mud losses in depleted zones
- Potential elimination of at least one liner string
- Mitigation of risk

Figure 12 illustrates the process. The use of a triple deck high performance shaker fully supports these new fluid formulations by collecting the sized particles from the middle deck prior to screening the drilling fluid on the lower deck for removal of fine drilled solids. Screen selection considerations are determined by hole size, interval length and drilling fluid parameters.

Case History

An operator planned a challenging 7 ½-in. sidetrack in the Gulf of Mexico, which consisted of highly depleted sandstone. The risk of mud losses, differentially stuck pipe and sticking the production liner off bottom was the concern.

A constant rheology synthetic drilling fluid was chosen to drill the sidetrack. After temperature modeling was performed to determine circulating temperature profiles, the fluid viscosity measurements were tested under the expected downhole pressure and temperature conditions. Hydraulics modeling was then performed at the anticipated flow rates to predict maximum downhole pressures.

Review of available offset information including logging while drilling and wire line logs, hydraulic fracturing reports, LOTs, mud reports and daily drilling reports was conducted to estimate rock strength and formation stresses.

A geomechanics analysis indicated near wellbore fracturing was likely to occur. Based on the fracture

characterization, the bridging software was used to select the proper wellbore strengthening products while drilling through the depleted sandstone.

Rigsite execution plans included the following recommendations:

- Add a specified concentration of wellbore strengthening material to the active system prior to drilling the depleted zone.
- Set up a schedule to replenish material while drilling the depleted zone.
- Maintain a constant rate of penetration (ROP) while drilling through the depleted zone.
- Maintain an ECD value within the preplanned value.
- Screen shakers to ensure bridging material remained in the system while drilling the depleted zone.

More than 100 ft of depleted sandstone was drilled in the interval with an ECD of 1.1 ppg above the estimated fracture gradient. The sidetrack was successfully drilled with no downhole losses or stuck pipe while drilling and/or running and cementing the production liner.

Conclusions

An integrated approach to wellbore stability is presented. By coupling temperature, hydraulics, geomechanics and bridging software, a comprehensive analysis in the pre-planning and execution stage of a drilling project can provide an operator the valuable information to help eliminate NPT.

A case history was presented, which demonstrates the technique of an integrated approach to deliver improved wellbore stability.

Acknowledgments

The author's would like to thank Baker Hughes Incorporated for permission to publish this paper. Additionally we thank Bill Bradford and Timothy Edwards from Baker Hughes, and Dan VanOrden with Resource Data Incorporated.

References

1. Alberty, M.W. and McLean M.R. "A Physical Model for Stress Cages," SPE 90493, SPE Annual Technology Conference, Houston, Texas, September 26-29, 2004.
2. Aston, M.S. Alberty, M.W., de Jong, H.J. and Armagost, K. "Drilling Fluids for Wellbore Strengthening," SPE 87130, IADC/SPE Drilling Conference, Dallas, Texas, March 2-4, 2004.
3. Benaissa, S., Bachelot A. and Ong S. "Preventing Mud Losses and Differential Sticking by Altering Effective Stress of Depleted Sands," IADC/SPE 103816, IADC/SPE Asia Pacific Drilling Technology Conference and Exhibition, Bangkok, Thailand, November 13-15, 2006.
4. Jones, J.F., Taylor, G.D. and Barree, R.D. "Successfully Managing Drilling-Fluid Losses in Multiple Highly Depleted Sands," OTC 13107, Offshore Technology Conference, Houston, Texas, April 30 - 3 May 4, 2001.
5. Gonzalez, M.E., Bloys, J.B., Lofton, J.E., Pepin G.P., Schmidt, J.H., Naquin, C.J. Ellis, S.T., Laursen, P.E. "Increasing Effective Fracture Gradients by Managing Wellbore Temperatures," IADC/SPE 87217, IADC/SPE Drilling Conference, Dallas, Texas, March 2-4, 2004.
6. Davison, J.M., Clary, S., Saasen, A., Allouche, M., Bodin, D., Nguyen, V-A. "Rheology of Various Drilling Fluid Systems Under Deepwater Drilling Conditions and the Importance of Accurate Predictions of Downhole Fluid Hydraulics," SPE 56632, SPE Annual Technical Conference, Houston, Texas, Oct 3-6, 1999.
7. Peters, E.J., Chenevert, M.E. and Zhang, C. "A Model for Predicting the Density of Oil Muds at High Pressure and Temperature," SPE 18036, SPE Annual Technical Conference and Exhibition, Houston, Texas, October 2-5, 1988.
8. Kemp, N.P., Thomas, D.C., Atkinson, G. and Atkinson, B. "Density Modeling for Brines as a Function of Composition, Temperature, and Pressure." *SPE Production Engineering*, (November 1989) 394-400.
9. Vefring, E.H., Anfinsen, B., Bjorkevoll, K.S. and Rommetveit R. "Simulator accurately predicts conditions in HPHT Wells." *Oil & Gas Journal* (Oct. 10, 1994) 77-80.
10. Mullen, G., Singamsetty, C., Dye, W., Ledet, D., Rawicki, A., Robichaux, T.J., Authement, G. "Planning and Field Validation of Annular Pressure Predictions," AADE 01-NC-HO-08, AADE National Drilling Conference, Houston, Texas, March 27-29, 2001.
11. Vickers, S., Cowie, M., Jones, T. and Twynam, A. "A New Methodology that Surpasses Current Bridging Theories to Efficiently Seal a Varied Pore Throat Distribution as Found in Natural Reservoir Formations," AADE-06-DF-HO-16, AADE Fluids Conference, Houston, Texas, April 11-12, 2006.

Table 1: Input Parameters and Results

| Input Parameters | Results |
|---------------------------------|---|
| Pore pressure | Overburden |
| S_V gradient | Pore pressure |
| S_h / S_H horizontal stresses | S_h / S_H |
| Azimuth of S_H | Formation breakdown pressure vertical and directional |
| Wellbore information | Maximum wellbore pressure (ECD) |
| Geothermal gradient* | Collapse pressure |
| Mud temperature* | Fracture pressure |
| ESD / ECD | Formation temperature |
| Poisson's ratio | Formation / wellbore temperature difference |
| Biot's constant | Dynamic fracture net pressure |
| Young's modulus | Maximum fracture width |
| Cohesion or UCS | Average fracture width |
| Internal friction angle | Static crush pressure |
| Tensile strength | Static maximum fracture width |
| | Fracture width variation |

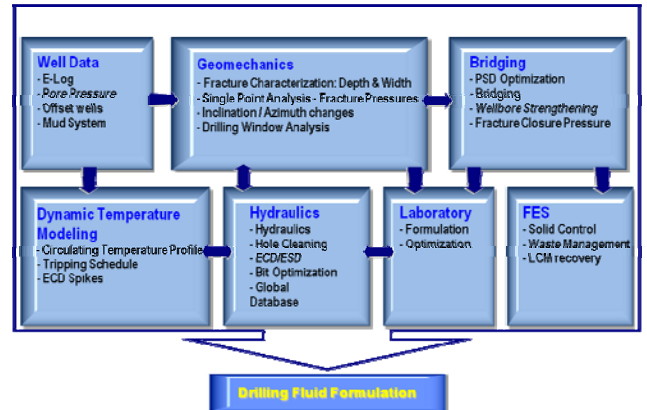


Figure 1: Integrated solutions diagram

Table 2: LTMO PVT Data

| PSI | Temperature, °F | | | | | | |
|-------|-----------------|------|------|------|------|------|------|
| | 62 | 100 | 150 | 200 | 250 | 300 | 350 |
| 15 | 6.75 | 6.63 | 6.48 | 6.34 | 6.20 | 6.06 | 5.92 |
| 1000 | 6.78 | 6.67 | 6.52 | 6.38 | 6.24 | 6.10 | 5.97 |
| 5000 | 6.91 | 6.81 | 6.67 | 6.54 | 6.41 | 6.29 | 6.16 |
| 10000 | 7.05 | 6.96 | 6.84 | 6.72 | 6.60 | 6.49 | 6.38 |
| 15000 | 7.16 | 7.07 | 6.97 | 6.86 | 6.76 | 6.66 | 6.57 |
| 20000 | 7.24 | 7.16 | 7.07 | 6.98 | 6.89 | 6.81 | 6.73 |

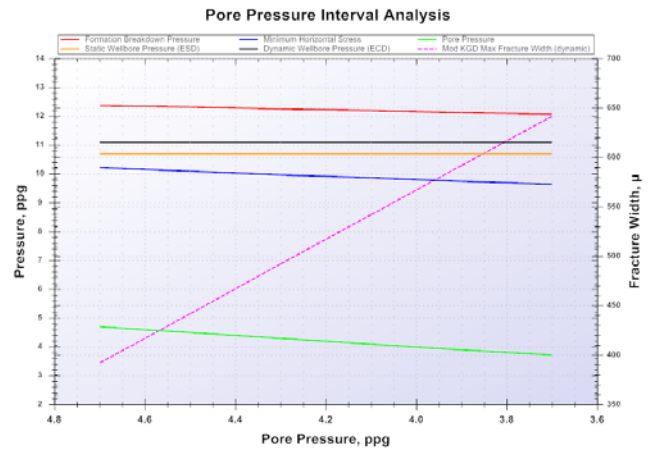


Figure 2: Pore pressure uncertainty

Table 3: Whole Mud Density

| PSI | Temperature, °F | | | | | | |
|-------|-----------------|-------|-------|-------|-------|-------|-------|
| | 62 | 100 | 150 | 200 | 250 | 300 | 350 |
| 15 | 11.34 | 11.25 | 11.14 | 11.03 | 10.92 | 10.81 | 10.70 |
| 1000 | 11.37 | 11.28 | 11.17 | 11.06 | 10.95 | 10.84 | 10.74 |
| 5000 | 11.47 | 11.39 | 11.28 | 11.18 | 11.08 | 10.98 | 10.88 |
| 10000 | 11.57 | 11.50 | 11.40 | 11.31 | 11.22 | 11.12 | 11.04 |
| 15000 | 11.66 | 11.59 | 11.51 | 11.42 | 11.34 | 11.25 | 11.17 |
| 20000 | 11.73 | 11.67 | 11.59 | 11.51 | 11.44 | 11.36 | 11.29 |

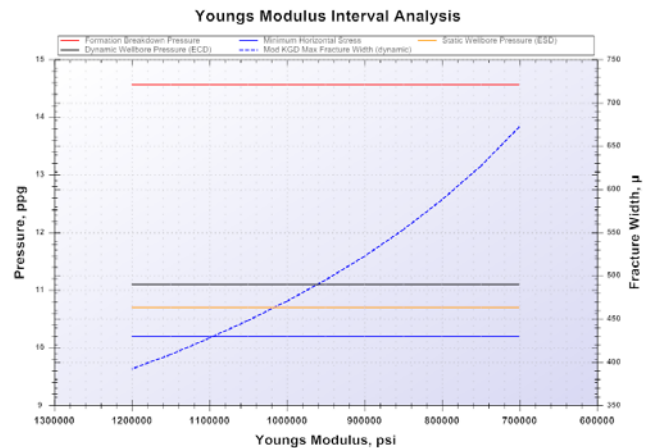


Figure 3: Young's modulus uncertainty

| Radial Formation Stress Distribution | Hoop Stress Distribution | | Drillability Matrix Max ECD | | Drillability Matrix Max ESD | | | |
|--------------------------------------|--------------------------|-------|-----------------------------|-------|-----------------------------|-------|-------|-------|
| | 270 | 271 | 272 | 273 | 274 | 275 | 276 | 277 |
| 25 | 11.78 | 11.78 | 11.78 | 11.78 | 11.78 | 11.79 | 11.79 | 11.8 |
| 26 | 11.69 | 11.69 | 11.69 | 11.69 | 11.69 | 11.7 | 11.7 | 11.71 |
| 27 | 11.59 | 11.59 | 11.59 | 11.59 | 11.6 | 11.6 | 11.61 | 11.61 |
| 28 | 11.49 | 11.49 | 11.49 | 11.5 | 11.5 | 11.5 | 11.51 | 11.52 |
| 29 | 11.39 | 11.39 | 11.4 | 11.4 | 11.4 | 11.4 | 11.41 | 11.42 |
| 30 | 11.29 | 11.29 | 11.29 | 11.3 | 11.3 | 11.3 | 11.31 | 11.31 |
| 31 | 11.19 | 11.19 | 11.19 | 11.19 | 11.19 | 11.2 | 11.2 | 11.21 |
| 32 | 11.08 | 11.08 | 11.08 | 11.09 | 11.09 | 11.09 | 11.1 | 11.1 |
| 33 | 10.97 | 10.97 | 10.98 | 10.98 | 10.98 | 10.98 | 10.99 | 11 |
| 34 | 10.86 | 10.86 | 10.87 | 10.87 | 10.87 | 10.88 | 10.88 | 10.89 |
| 35 | 10.75 | 10.75 | 10.75 | 10.76 | 10.76 | 10.76 | 10.77 | 10.78 |
| 36 | 10.64 | 10.64 | 10.64 | 10.64 | 10.65 | 10.65 | 10.66 | 10.66 |
| 37 | 10.53 | 10.53 | 10.53 | 10.53 | 10.53 | 10.54 | 10.54 | 10.55 |
| 38 | 10.41 | 10.41 | 10.41 | 10.42 | 10.42 | 10.42 | 10.43 | 10.44 |
| 39 | 10.3 | 10.3 | 10.3 | 10.3 | 10.3 | 10.31 | 10.31 | 10.32 |
| 40 | 10.19 | 10.19 | 10.19 | 10.19 | 10.19 | 10.19 | 10.2 | 10.2 |
| 41 | 10.19 | 10.19 | 10.19 | 10.19 | 10.19 | 10.19 | 10.19 | 10.19 |
| 42 | 10.19 | 10.19 | 10.19 | 10.19 | 10.19 | 10.19 | 10.19 | 10.19 |
| 43 | 10.19 | 10.19 | 10.19 | 10.19 | 10.19 | 10.19 | 10.19 | 10.19 |
| 44 | 10.19 | 10.19 | 10.19 | 10.19 | 10.19 | 10.19 | 10.19 | 10.19 |
| 45 | 10.19 | 10.19 | 10.19 | 10.19 | 10.19 | 10.19 | 10.19 | 10.19 |

Figure 4: Drillability matrix

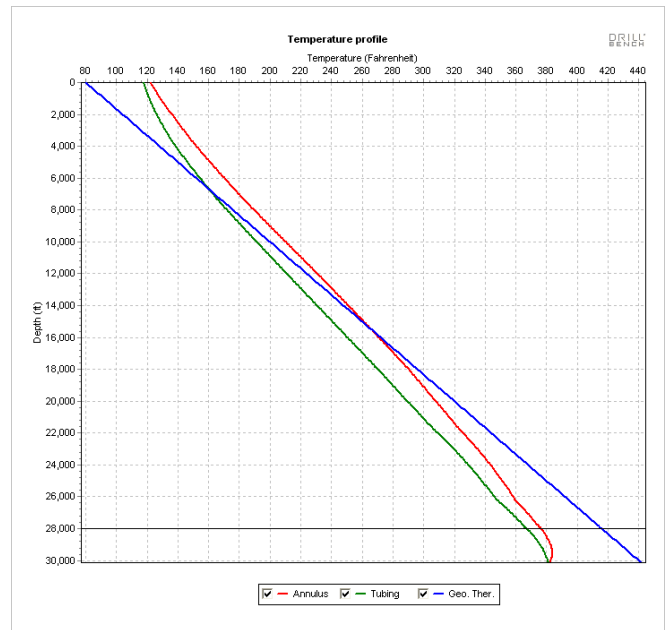


Figure 6: Circulating temperature profile

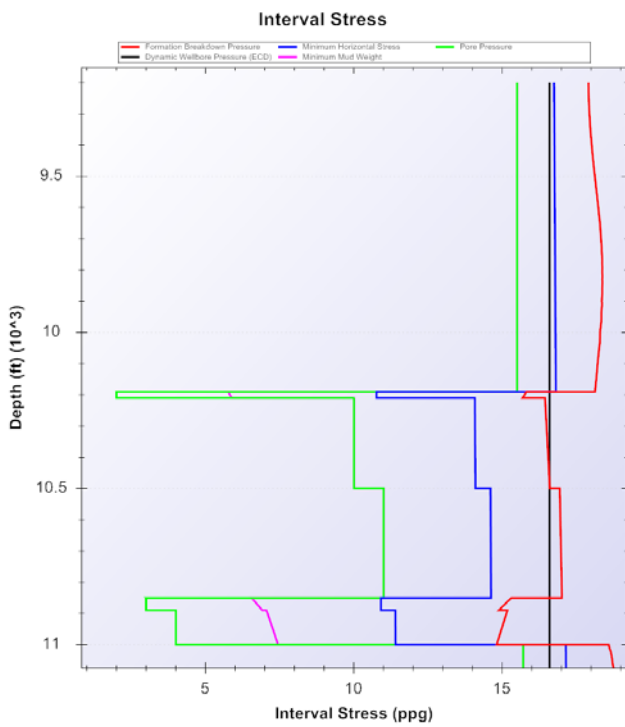


Figure 5: Interval analysis

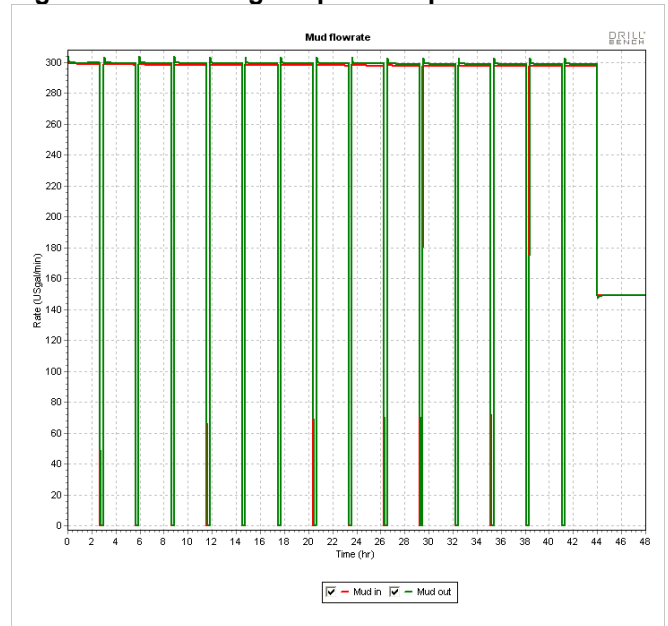


Figure 7: Connections (pumps on, pumps off)

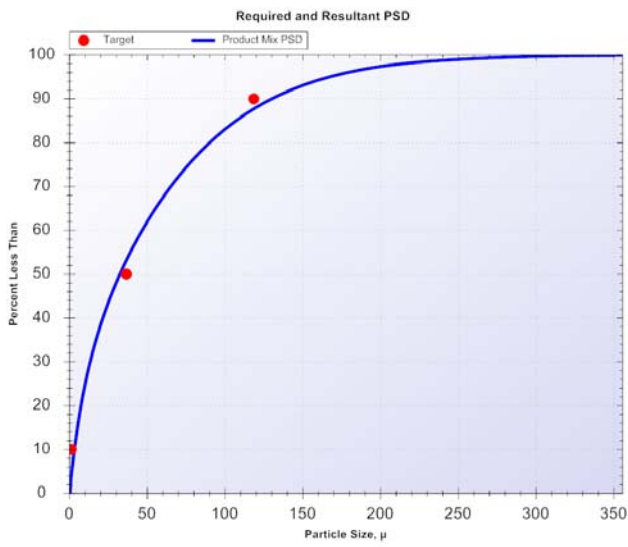


Figure 8: Bridging results w/o mud PSD

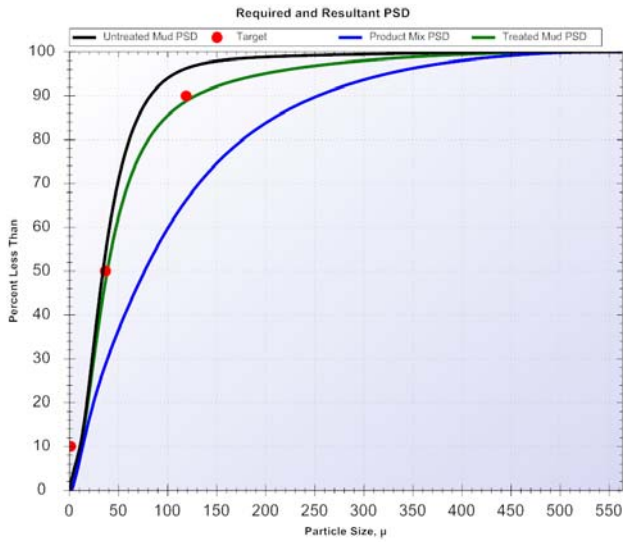


Figure 9: Bridging results with mud PSD



Figure 10: Slot assembly top view

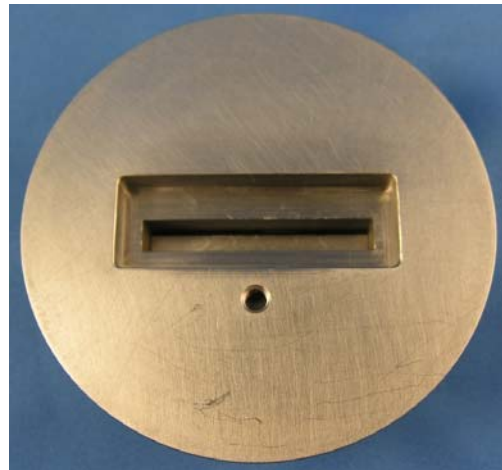


Figure 11: Slot assembly bottom view

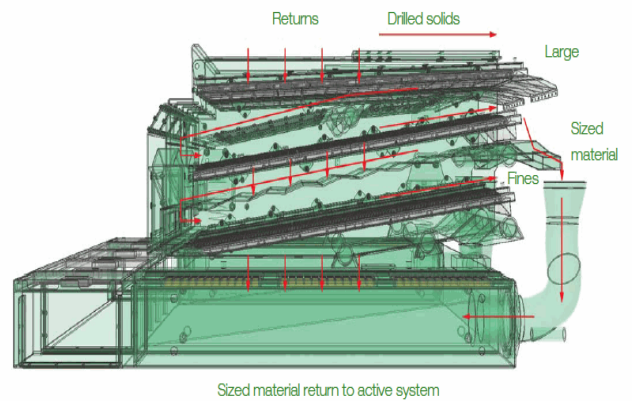


Figure 12: LCM recovery system